

LETTER TO THE EDITOR

Penumbral models in the light of Hinode spectropolarimetric observations

J. Jurčák^{1,2} and L.R. Bellot Rubio^{1,3}

¹ National Astronomical Observatory of Japan, 2-21-1 Osawa, Mitaka, Tokyo 181-8588, Japan

² Astronomical Institute of the Academy of Sciences, Fricova 298, 25165 Ondřejov, Czech Republic

³ Instituto de Astrofísica de Andalucía (CSIC), Apdo. Correos 3004, 18080 Granada, Spain

Received September 15, 1996; accepted March 16, 1997

ABSTRACT

Aims. The realism of current models of the penumbra is assessed by comparing their predictions with the plasma properties of penumbral filaments as retrieved from spectropolarimetric observations.

Methods. The spectropolarimeter onboard Hinode allows us to distinguish for the first time the fine structure of the penumbra. Therefore, we can use one-component inversions to obtain the stratifications of plasma parameters in each pixel. The correlations between the plasma parameters and the continuum intensity are studied.

Results. We find that, in the outer penumbra, the stronger flows are located in dark filaments. This finding does not seem to be compatible with the scenario of a field-free gappy penumbra.

Key words. Sun: sunspots – Sun: photosphere – Techniques: polarimetric

1. Introduction

There are two models of the penumbral fine structure under discussion nowadays. The first one is the uncombed model proposed by Solanki & Montavon (1993) and further developed by Martínez Pillet (2000) to explain the broad-band circular polarisation observed in sunspots. It envisages the penumbra as a collection of horizontal flux tubes embedded in a more vertical and stronger background field. Schlichenmaier et al. (1998) made simulations of the temporal evolution of such flux tubes. Starting at the sunspot magnetopause, they rise by magnetic buoyancy and quickly become horizontal in the photosphere. At the same time, a strong Evershed flow develops due to the gas pressure gradient that builds up during the rise. The tubes are hotter than the surrounding plasma and appear as bright penumbral filaments which gradually cool down due to radiative losses, i.e. become dark further from the bright penumbral grains where the tubes cross the $\log \tau = 0$ layer. Hereafter, this model will be called the rising flux tube model (RFT).

The second model was suggested by Spruit & Scharmer (2006). These authors argued that the RFT model cannot produce sufficient heating of the penumbra. As an alternative, they proposed a field-free gap model (FFG) which consists of field-free material protruding into the penumbral magnetic field from below. With such a configuration, the bright filaments would be heated all along their lengths and not only at the point of emergence as in the case of the RFT model. While the FFG model does not offer any explanation for the Evershed flow, there is only one place where the flow can reside, namely on top of the field free gaps, since this is the sole region in the model where horizontal fields exist.

Both models have problems from a theoretical point of view which need to be clarified (see Bellot Rubio, 2007, and references therein). However, as illustrated in Fig. 1, RFTs and FFGs should produce similar stratifications of the plasma parameters

if they are placed near $\log \tau = 0$ (marked by the gray line). The two models predict weaker and more inclined magnetic fields low in the atmosphere, along with an increase of the line-of-sight (LOS) velocity. Indeed, this is what Jurčák et al. (2007) found in the bright filaments of the inner penumbra from an analysis of Hinode spectropolarimetric (SP) data.

In this Letter we concentrate on the middle and outer penumbra where differences between the models could be more pronounced from an observational point of view. According to the FFG model, weak and horizontal magnetic fields coupled with increased LOS velocities should be found in bright areas everywhere in the penumbra. By contrast, the RFT model expects such characteristics in the dark filaments of the outer penumbra.

2. Observations and inversion technique

The data analysed here were obtained using the SP (Tarbell et al., 2007), one of the focal-plane instruments of the Solar Optical

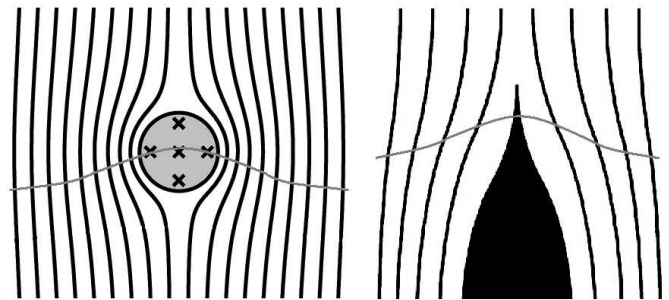


Fig. 1. Sketch of a RFT (left) and a FFG (right) surrounded by the background magnetic field of the penumbra. The gray line represents the possible position of the optical depth unity layer.

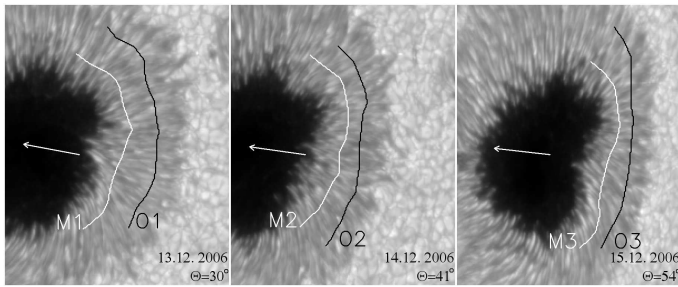


Fig. 2. Maps of continuum intensity at 630.2 nm reconstructed from the SP raster scans. North is up and West to the right. The maps cover the limb side part of the penumbra in evolving AR 10930. The arrows point to the disc centre. The black and white lines represent the paths selected for analysis.

Telescope (Tsuneta et al., 2007) onboard the Hinode satellite (Kosugi et al., 2007). This instrument measures the Stokes profiles of the two iron lines at 630.15 nm and 630.25 nm.

Normal SP scans of AR 10930, providing a spatial resolution of $0''.32$ and a noise level of $10^{-3}I_c$, were taken on December 13, 14, and 15, 2006. These days the spot was located far from the disc centre (heliocentric angles θ of 30° , 41° , and 54°). The three panels of Fig. 2 show the limb-side part of AR 10930 as reconstructed from the intensities observed in the red continuum of the 630.25 nm line. The Stokes V profiles emerging from the penumbra show significant area asymmetries due to the existence of gradients of the plasma parameters in the line-forming region. We can clearly see the bright and dark filaments in the continuum maps. Their signals are not mixed up as in the case of ground-based observations, implying that the penumbral fine structure is distinguished in spectropolarimetric measurements for the first time.

Each day we selected two paths through the penumbra. As can be seen in Fig. 2, one of the paths is located in the inner-middle part of the penumbra and the second in the outer part. The paths were chosen so as to minimise any trend of the continuum intensity along them, except for small-scale fluctuations caused by the alternating bright and dark filaments.

The observations and data reduction are described in detail in Jurčák et al. (2007). The zero point of the velocity scale is taken to be the line core position of the mean quiet Sun intensity profile, computed separately for each slit. The observed Stokes spectra have been inverted using the SIRGAUS code (Bellot Rubio, 2003), which is a modified version of SIR (Ruiz Cobo & del Toro Iniesta, 1992). This code presumes the existence of a Gaussian perturbation (GP) in the stratifications of plasma parameters somewhere in the line-forming region. Given the high angular resolution of the Hinode measurements, we only consider one-component model atmospheres.

In total, the inversion code looks for the best solution in a space of 13 free parameters. Six of them define the physical conditions of the unperturbed atmosphere: two for the temperature (T), and one for the field strength (B), inclination (γ), azimuth (ϕ), and LOS velocity (v_{LOS}). The width and position of the GP is the same for all plasma parameters, which adds two more free parameters. The rest of parameters are the amplitudes of the perturbation in the different physical quantities. As initial values we adopt $\Delta T = +800$ K, $\Delta B = -500$ G, $\Delta\gamma = -30^\circ$, $\Delta\phi = -5^\circ$, and $\Delta v = +3$ km s $^{-1}$. Depending on the position of the perturbation, these values can represent either the conditions of a RFT or those of a FFG. For more details, the reader is referred to Jurčák et al. (2007).

3. Choice of plasma parameters

As discussed by Jurčák et al. (2007), the inversion results are not completely unambiguous in the mid and outer penumbra, i.e., the targets of the present study. Figure 3 displays the Stokes I and V profiles observed in one of the pixels of cut O1 (solid lines). The dashed and dotted lines represent two fits obtained by the inversion code. The corresponding stratifications of magnetic field strength, inclination, and LOS velocity are shown in the left part of Fig. 3.

Although the stratifications are significantly different, they share some similarities. The sign and amplitude of the GP for the LOS velocity and the magnetic field inclination are almost independent of the height of the Gaussian. Variations in the position of the GP mainly change the amplitude and sign of the magnetic field strength perturbation. Which of these solutions is closer to reality can be hardly decided on the basis of the merit function (sum of squared differences between observed and synthetic profiles), as they are usually of comparable value.

Since the height of the GP is not well constrained, we decided to rely on the part of the solution which is similar for both possibilities, i.e. the maximal LOS velocity obtained in the line-forming region (between $\log \tau = 0$ and -3 , as the lines are not very sensitive to the plasma properties higher or lower in the atmosphere, cf. Cabrera Solana et al. 2005). If the centre of the GP is located outside of this optical depth range, we use the maximum value reached at the lower or upper boundary. As an example, the stratification represented by the dotted line in Fig. 3 would get a LOS velocity of 5.2 km s $^{-1}$ (filled circle). When the peak of the perturbation is inside the line-forming region, we do not use the amplitude of the GP because it may be overestimated. Rather, we decrease it by a factor which depends on the width of the perturbation: the narrower the GP, the more is the amplitude reduced. The dashed lines in Fig. 3 provides an example of this situation. The value adopted for the LOS velocity is not the amplitude of the GP (7.5 km s $^{-1}$), but 4.5 km s $^{-1}$ (black square). Such a reduction of the velocity peak by a factor of 0.6 is appropriate for a GP with a HWHM of 0.3 (in units of $\log \tau$).

4. Results

Figure 4 shows the values of the LOS velocity (solid lines) along the six paths selected for analysis. The individual cuts have been labelled as in Fig. 2. The dashed lines represent the continuum intensity along the paths. The correlation between LOS velocities and continuum intensities can be used to validate the two models of the penumbral fine structure.

In Fig. 4, the LOS velocity increases from left to right or, equivalently, with heliocentric angle. We find mean values of 3.7 km s $^{-1}$, 5.4 km s $^{-1}$, and 5.9 km s $^{-1}$ for cuts M1, M2, and M3 and 4.5 km s $^{-1}$, 6.6 km s $^{-1}$, and 7.4 km s $^{-1}$ for cuts in the outer penumbra. The increase in LOS velocity between cuts M1–M3 (O1–O3) is simply the consequence of projection effects (the angle between the line of sight and the flow vector becomes smaller as the spot moves away from the disc center). The increase in mean LOS velocity between the middle and outer penumbra confirms previous reports of enhanced flow velocity with increasing distance from the umbra (e.g., Rimmele, 1995; Westendorp Plaza et al., 2001; Solanki, 2003). This behaviour is also predicted by simulations of moving penumbral tubes (Schlichenmaier et al., 1998).

The decrease in continuum intensity between cuts M1–M3 and O1–O3 is a consequence of limb darkening. As we compute the correlation coefficients individually for each cut, these trends

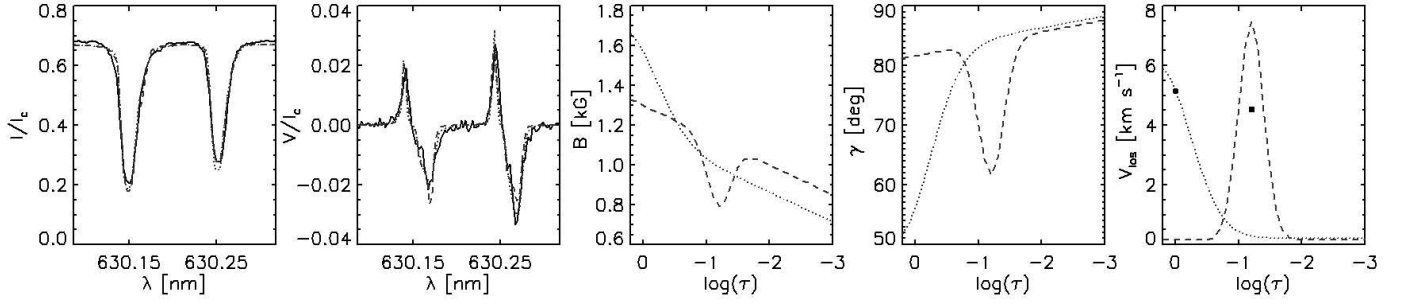


Fig. 3. Stokes I and V profiles observed in a pixel of cut O1 (solid lines) with two different fits (dashed and dotted lines) and their corresponding stratifications of magnetic field strength, inclination, and LOS velocity.

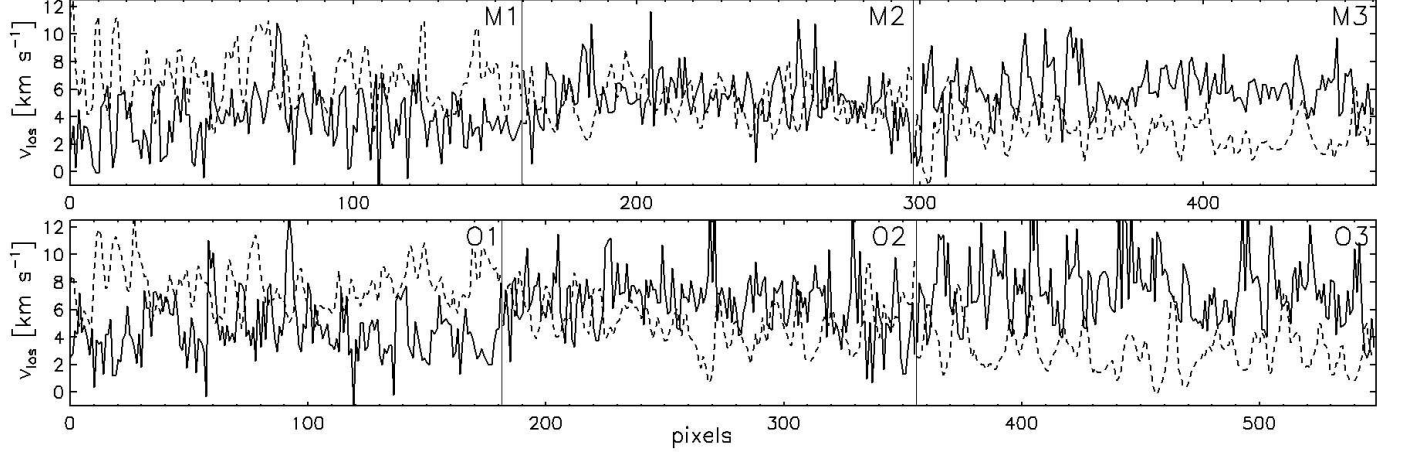


Fig. 4. Inferred values of the LOS velocity (solid lines) along the six cuts displayed in Fig. 2. Positive velocities correspond to redshifts. The dashed lines represent the continuum intensity along the cuts, normalised to the quiet Sun continuum intensity.

Table 1. Correlation coefficients between the LOS velocity (v_{LOS}) and continuum intensity (I_c , left column), inclination (γ , middle column), and magnetic field strength (B , right column).

Cut	v_{LOS} vs. I_c	v_{LOS} vs. γ	v_{LOS} vs. B
M1	-0.132	0.312	-0.533
M2	-0.437	0.767	-0.636
M3	-0.340	0.696	-0.652
O1	-0.508	0.799	-0.325
O2	-0.506	0.639	-0.321
O3	-0.302	0.671	0.095

do not have any effect on the resulting values. The main concern was to avoid significant trends in continuum intensity along one particular path, since this would influence the resulting correlation coefficient. As demonstrated by the dashed lines of Fig. 4, the intensity changes we observe are mostly due to the dark and bright filaments, with global trends being negligible in all cuts.

Table 1 summarises the correlation coefficients obtained for the six cuts. The values corresponding to the continuum intensity vs LOS velocity show that the strongest flows are associated with dark filaments in the mid and outer penumbra. In three out of six cases we obtain absolute values larger than 0.4, which is quite high compared to previous analyses. The relation between these parameters has been studied by many authors (see e.g. Rimmele, 1995; Westendorp Plaza et al., 2001; Solanki, 2003) with various results. Recently, Langhans et al. (2005) found the highest LOS velocities to occur in dark filaments everywhere in the penumbra, although they did not evaluate correlation co-

efficients. Schlichenmaier et al. (2005) found the LOS velocities to be associated with bright and dark filaments in the inner and outer penumbra, respectively. The work of Hirzberger et al. (2005) confirms the existence of strong flows in bright filaments, but only near their innermost footpoints (the so-called bright penumbral grains). Rimmele & Marino (2006), from an analysis of diffraction-limited Dopplergrams, concluded that the Evershed flow appears in the bright penumbral grains as an up-flow and rapidly (within $1''$) turns into a horizontal flow residing in dark filaments. From spectropolarimetric measurements, Jurčák et al. (2007) also detected increased LOS velocities in bright filaments protruding into the umbra.

Only M1 does not show a clear relation between LOS velocity and brightness. This cut is the one closest to the umbral/penumbral boundary (Fig. 2) and shows many more pixels with negligible velocities than the other cuts (Fig. 4). Since the flow is correlated with bright filaments in the innermost penumbra (Schlichenmaier et al., 2005; Hirzberger et al., 2005; Jurčák et al., 2007) and with dark filaments in the mid and outer penumbra (as we are trying to prove here at the resolution of Hinode), there must be a place where the correlation changes sign. Consequently, the correlation coefficient has to drop to zero somewhere in the inner penumbra, and M1 could be close to that region.

Figure 4 also demonstrates that there are very few areas with small values of the LOS velocity. Such places occur more frequently in the case of cut M1 and tend to correspond to local brightenings in the continuum intensity curves. The lack of zero flow velocities represents another problem for the FFG model (if the fine structure is distinguished, as we claim). By contrast, this

observational result is easily explained using the RFT model, as it predicts flows in both bright and dark regions, the later being the darkened tails of RFTs.

The other columns of Table 1 quantify the relation between the LOS velocity and the magnetic field inclination and strength. It is generally accepted that the Evershed flow resides in areas of horizontal fields. The second column of Table 1 just confirms this fact. The third column shows that the flow is associated with weaker magnetic fields, although the correlation coefficients decrease significantly from the mid to the outer penumbra. This implies a smaller difference in magnetic field strength between flow channels and the surrounding atmosphere in the outer penumbra, which is not surprising as both the RFT and FFG models predict an equalisation of the field strength with increasing distance from the umbra. In the case of the RFT model, the equalisation is a real physical process, whereas in the case of the FFG model it is only apparent. The smaller field strength difference between flow channels and surrounding plasma has also been inferred from two-component Stokes inversions (see e.g. Bellot Rubio et al., 2004; Borrero et al., 2006) and analyses of the net circular polarisation observed in the penumbra at high angular resolution (Tritschler et al., 2007).

5. Discussion and conclusions

We consider the negative correlation between continuum intensity and LOS velocity as the most important result of our analysis. It implies that the stronger flows are localised in dark filaments in the middle and outer penumbra. A similar conclusion has been reached by Schlichenmaier et al. (2005) and Ichimoto et al. (2007) from simpler interpretations of filtergrams and spectropolarimetric data, respectively. This finding is in contradiction with the FFG model, as it predicts that the flow should be associated with bright filaments everywhere in the penumbra. Such a relation seems to hold only in the innermost penumbra.

The correlation coefficients between LOS velocity and magnetic field inclination presented in this Letter confirm that the flow is confined to the horizontal fields. In the mid and outer penumbra, the average values of γ in the flow channels are 97° and 74° , respectively. Since γ is measured with respect to the local vertical and the spot is of negative polarity, the flow channels are inclined upward in the mid penumbra ($+7^\circ$ with respect to the surface) and diving in the outer penumbra (-16°). The existence of magnetic field lines pointing to the solar interior in the outer penumbra represents another problem for the FFG model (Bellot Rubio, 2007). We also observe a decrease in the correlation between LOS velocity and field strength with increasing distance from the umbra. We suggest that this decrease is due to field strengths becoming more similar in the flow channels and the surrounding atmosphere as the outer penumbral boundary is approached.

The RFT simulations of Schlichenmaier et al. (1998) seem to be able to explain all the results of our analysis, including the sign reversal of the correlation between LOS velocity and brightness from the innermost penumbra to the mid (outer) penumbra, the larger mean value of the LOS velocity in the outer penumbra as compared with that in the mid penumbra, and the absence of areas with zero LOS velocities in the mid and outer penumbra. The agreement between the plasma parameters predicted by the RFT simulations and those derived from the inversion of Hinode measurements favours the RFT model over the FFG model.

Acknowledgements. This work has been enabled thanks to the funding provided by the Japan Society for the Promotion of Science. Hinode is a Japanese mission developed and launched by ISAS/JAXA, with NAOJ as domestic partner

and NASA and STFC (UK) as international partners. It is operated by these agencies in co-operation with ESA and NSC (Norway). The computations were carried out at the NAOJ Hinode Science Center, which is supported by the Grant-in-Aid for Creative Scientific Research The Basic Study of Space Weather Prediction from MEXT, Japan (Head Investigator: K. Shibata), generous donations from Sun Microsystems, and NAOJ internal funding. Financial support from the Spanish Ministerio de Educación y Ciencia through project ESP2006-13030-C06-02 is gratefully acknowledged.

References

- Bellot Rubio, L. R. 2003, ASP Conf. Series, 307, 301
 Bellot Rubio, L.R. 2007, in: Highlights of Spanish Astrophysics IV, eds. F. Figueras et al. (Dordrecht: Springer), 271
 Bellot Rubio, L. R., Balthasar, H., & Collados, M. 2004, A&A, 427, 319
 Borrero, J. M., Solanki, S. K., Lagg, A., Socas-Navarro, H., & Lites, B. 2006, A&A, 450, 383
 Cabrera Solana, D., Bellot Rubio, L.R., & del Toro Iniesta, J.C. 2005, A&A, 439, 687
 Hirzberger, J., Stangl, S., Gersin, K., et al. 2005, A&A, 442, 1079
 Ichimoto, K., et al. 2007, PASJ, 59, in press
 Jurčák, J., et al. 2007, PASJ, 59, in press [astro-ph/0707.1560]
 Kosugi, T., et al. 2007, Sol. Phys., 243, 3
 Langhans, K., Scharmer, G. B., Kiselman, D., Löfdahl, M. G., & Berger, T. E. 2005, A&A, 436, 1087
 Martínez Pillet, V. 2000, A&A, 361, 734
 Rimmele, T. R. 1995, A&A, 298, 260
 Rimmele, T., & Marino, J. 2006, ApJ, 646, 593
 Ruiz Cobo, B. & del Toro Iniesta, J. C. 1992, ApJ, 398, 375
 Schlichenmaier, R., Jahn, K., & Schmidt, H. U. 1998, A&A, 337, 897
 Schlichenmaier, R., Bellot Rubio, L. R., & Tritschler, A. 2005, AN, 326, 301
 Solanki, S. K. 2003, A&A Rev., 11, 153
 Solanki, S. K. & Montavon, C. A. P. 1993, A&A, 275, 283
 Spruit, H. C. & Scharmer, G. B. 2006, A&A, 447, 343
 Tarbell, T., et al. 2007, Sol. Phys., in preparation
 Tsuneta, S., et al. 2007, Sol. Phys., submitted
 Tritschler, A., Mueller, D. A. N., Schlichenmaier, R., & Hagenaar, H. J. 2007, ApJ, in press, [arXiv:0710.4545]
 Westendorp Plaza, C., del Toro Iniesta, J. C., Ruiz Cobo, B., & Martínez Pillet, V. 2001, ApJ, 547, 1148